VIA MEDICA

ORIGINAL ARTICLE

Folia Morphol.
Vol. 70, No. 4, pp. 228–234

ISSN 0015–5659
www.fm.viamedica.pl

The claustrum: three-dimensional reconstruction, photorealistic imaging, and stereotactic approach

S. Kapakin

Department of Anatomy, Faculty of Medicine, Atatürk University, Erzurum, Turkey

[Received 7 July 2011; Accepted 25 September 2011]

The purpose of this study was to reveal the computer-aided three-dimensional (3D) appearance, the dimensions, and neighbourly relations of the claustrum and make a stereotactic approach to it by using serial sections taken from the brain of a human cadaver. The Snake technique was used to carry out 3D reconstructions of the claustra and surrounding structures. The photorealistic imaging and stereotactic approach were rendered by using the Advanced Render Module in Cinema 4D software. The claustrum takes the form of the concavity of the insular cortex and the convexity of the putamen. The inferior border of the claustrum is at about the same level as the bottom edge of the insular cortex and the putamen, but the superior border of the claustrum is at a lower level than the upper edge of the insular cortex and the putamen. The volume of the right claustrum, in the dimensions of 35.5710 mm × 1.0912 mm × 16.0000 mm, was 828.8346 mm^3, and the volume of the left claustrum, in the dimensions of 32.9558 mm × 0.8321 mm × × 19.0000 mm, was 705.8160 mm^3. The surface areas of the right and left claustra were calculated to be 1551.149697 mm^2 and 1439.156450 mm^2 by using Surfdriver software. This is the first study reporting the 3D reconstruction and photorealistic imaging of the claustrum of the human brain. This technique enables us to determine the spatial coordinates of the target tissues and to rehearse the surgical procedures for preoperative trajectory planning by using virtual surgery. We believe that this study will be a really useful anatomic guide for neuroscientists and neurosurgeons interested in the claustrum. (Folia Morphol 2011; 70, 4: 228–234)

Key words: neuroanatomy, claustrum, three-dimensional reconstruction, photorealistic imaging, stereotactic approach, human brain

INTRODUCTION

The claustrum is a relatively thin band of grey matter in the lateral part of the cerebral hemisphere in mammals [14]. It is separated from the medially lying lentiform nucleus (putamen and globus pallidus) by the fibres of the external capsule and, in some mammals, from the laterally lying insular cortex by the fibres of the extreme capsule [25]. Through numerous neuroanatomical studies, the claustrum and many neocortical areas including the frontal cortex [33], visual cortical fields including the striate cortex [8], temporal cortex [56], entorhinal cortex [26], parieto-occipital cortex [51], and the parietal cortex [48] have been reported to be interconnected. Limbic structures such as the hippocampus [3] and the amygdala [4] as well as the caudate nucleus and putamen [6] regions have been shown to relate to dementia in Parkinson's disease [28, 29] are mutually connected to the claustrum [30].

Address for correspondence: S. Kapakin, Asst. Prof., Atatürk University, Faculty of Medicine, Department of Anatomy 25240 Erzurum, Turkey, tel:+90 442 231 6626, ext: 6626, fax:+90 442 236 0968, e-mail: sametkapakin@gmail.com

The claustrum's involvement in many higher-order cognitive functions such as fear recognition [54], experiential dread [12], memory storage [42], associative learning [15], repetitive behaviours including addiction [42, 45], multimodal processing in olfactory, auditory, visual, and tactile information, as well as emotional and behavioural responses [11], cognitive impairment [20], suppression of natural urges [36], seizures [58], and psychosis [52] is due to its ontogeny, proximity to the basal ganglia, amygdala, and insula, and reciprocal connections [19]. Crick and Koch [18] have also recently suggested that the claustrum may contain specialised mechanisms that permit information to travel widely within its anterior–posterior and ventral-dorsal extent to synchronise different perceptual, cognitive, and motor modalities.

The structure and function of the claustrum are enigmatic, consistent with the derivation of its name "a hidden place". The claustrum is present in the forebrain of arguably all mammals [7, 34], but the exact structural boundaries of the claustrum have long puzzled investigators [38]. Most people working on the brain have heard of the claustrum — it was known to Ramon and Cajal — but very few have any idea what it does. It is thin and fairly small — in humans, its volume is a quarter of one percent of that of the cerebral cortex [34] — and so it is easily overlooked. In 1994, Crick [17] described the claustrum briefly, but since then we have left it to one side [18]. Despite the later use of various imaging methods, its shape could not go beyond the drawings based on two-dimensional (2D) sections. It was therefore aimed to reveal a computer-aided 3D appearance, the dimensions, and neighbourly relations of the claustrum and make a stereotactic approach to it by using serial sections taken from the brain of a human cadaver.

MATERIAL AND METHODS

Cryosectional image acquisition and features

The imaging data from the Visible Human Dataset, which is part of the Visible Human Project (VHP) initiated by the National Library of Medicine (NLM), were used. Visible Human Data exists in different modalities: computed tomography (CT), magnetic resonance imaging (MRI), and anatomical cryosections (Fig. 1A) [1]. To obtain the cryosection images, the cadaver was first frozen solid inside a large block of blue gel. Then, 1 mm-thick slices were successively cut away from an axial cross-section (planar cut perpendicular to the longitudinal axis of the body), and digital colour images were taken of each newly exposed cross-section. A total of 1,878 cryosection images were taken, spanning the body from head to toe. Each is in 24-bit colour and has a resolution of 1748 × 966 pixels [53].

Seventy-four cryosectional images were used to reconstruct the claustra and surrounding structures in order to reveal the morphology of the claustra and 3D spatial relationships among claustra and the surrounding structures on both sides (slice width = 600 mm, slice thickness = 1 mm, slice interval = 1). These cross-sections were between numbers 1067 and 1102, totally 36 cryosectional images, on the right side and between number 1069 and 1107, totalling 38 cryosectional images on the left side, where the claustra and its surrounding structures (insular cortex, putamen, and caudate nucleus) appeared and disappeared.

Reconstruction with the Snake technique, development of the photorealistic images and stereotactic approach

With this technique, the reconstruction process is defined in two steps, described as follows: at the first step, the user defines the organ contour on each slice. For that, one has to put a set of points around the organ on the slice. The Snake technique allows the polygon to fit exactly to the contour on the slice. This operation has to be done for every slice containing the organ. At the second step, once the elements have been interpreted and labelled on the different cross-sections as contours, the 3D reconstruction is performed by joining the contours of all the pertinent slices [23]. Initially the wire-frame (Fig. 1B) and the surface-rendered reconstructions were attained by the software. After generating a 3D surface model of the claustra and the surrounding structures, we converted the models to the DXF (Data Exchange File) format to render photorealistic imaging and stereotactic approach by using the Advanced Render Module in Cinema 4D software [31, 32].

RESULTS

The claustrum was a thin, irregular, odd-shaped, ribbon-like neuronal structure hidden between the insular cortex and the putamen. The claustrum took the form of the concavity of the insular cortex and the convexity of the putamen. While the claustrum covered the external surface of the putamen (Fig. 2A), it filled in the cavity of the insular cortex (Fig. 2B). The inferior border of the claustrum was at about the same level as the bottom edge of the insular cortex and the putamen, but the superior border of the claustrum was at a lower level than the upper

Table 1. Surface areas and volumes of the claustra and surrounding structures

Structures	Right side		Left side	
	Surface area [mm^2]	Volume [mm^3]	Surface area [mm^2]	Volume [mm^3]
Claustrum	1551.149697	828.834621	1439.156450	705.816094
Insular cortex	6281.884124	7920.608722	6188.577387	6649.799642
Putamen	2489.712768	4977.007858	2480.427290	4784.957815
Caudate nucleus	2691.199464	4658.697200	2667.030646	4527.521700

edge of the insular cortex and the putamen. As the claustrum was not the same size as the putamen and insular cortex, these structures did not match exactly. The main structure of the claustrum was in close contact with the main structures of the insular cortex and the putamen. It proved to be deployed in the best locality to provide the flow of the information among different regions of the brain and to be able to fulfil cognitive brain functions such as perception, attention, memory, language, executive functions, and problem-solving.

Surface areas and volumetric analyses of the claustra and surrounding structures are presented in Table 1. With morphometric evaluation of the claustrum reconstructions, on the right side the claustrum distances were 35.5710 mm longitudinally, 1.0912 mm laterally, and 16.0000 mm vertically. On the left side the claustrum distances were 32.9558 mm longitudinally, 0.8321 mm laterally, and 19.0000 mm vertically. The volumes of the right and left claustrum were 828.834621 mm^3 and 705.816094 mm^3, respectively. The surface areas of the right and left claustra were calculated to be 1551.149697 mm^2 and 1439.156450 mm^2, respectively, by using Surfdriver software. The mean distance between the right and the left claustra was 54.153 mm (Fig. 3A).

The mean distance values between the insular cortex and the claustrum were 1.18501 mm on the right side and 1.08040 mm on the left side (Fig. 2B). The mean distance values between the claustrum and the putamen were 0.91754 mm on the right side and 0.90355 mm on the left side (Fig. 2A). The claustra's spatial locations were 77.151 mm away from the anterior, 47.631 mm away from the lateral, and 98.445 mm away from the posterior on the right side and 80.838 mm away from the anterior, 48.928 mm away from the lateral, and 95.053 mm away from the posterior on the left side topologically (Fig. 3B).

This method enabled us to view the structures in different colours, in a studio environment, and from different angles. It was possible to move the structures in any direction individually or as a whole, which can be very useful for better understanding the spatial relationship of the mentioned structures and, therefore, can contribute to education, research, and surgery (Fig. 4). The technique also enables us to determine the spatial coordinates of the target tissues and to rehearse the surgical procedures for the preoperative trajectory planning by using virtual surgery. The data obtained from this method can be used to design instruments to be used in the operation (Fig. 5). To my knowledge, this is the first study reporting 3D reconstruction and photorealistic imaging of the claustrum of the human brain (Fig. 6).

DISCUSSION

The claustrum has been an overlooked neuroanatomical structure [19]. Although it has been studied by neuroanatomists for about two centuries [21], only one recent study has investigated the claustrum functionally [18]. The claustrum is present in all mammalian species [34] from the insectivore to man, though its precise shape and some of its connections appear to vary by species [18]. The claustrum is a prominent but ill-defined forebrain structure that has been suggested to integrate multisensory information and perhaps transform percepts into consciousness. The claustrum's shape and vague borders have hampered experimental assessment of its functions [38]. Segmentation of brain structures and tissues, especially in the subcortical regions, is very difficult due to limitations such as low-contrast, partial volume effects, and field inhomogeneities [9]. Although many methods have been proposed for subcortical structure segmentation, such tasks still remain challenging [2, 16]. Anatomical structures in the brain are related to neighbouring structures through their location, size, orientation, and shape. Neighbouring anatomical structures usually exhibit strong mutual spatial dependencies. An integration of these relationships into the segmentation process can provide improved accuracy and robustness [55, 57].

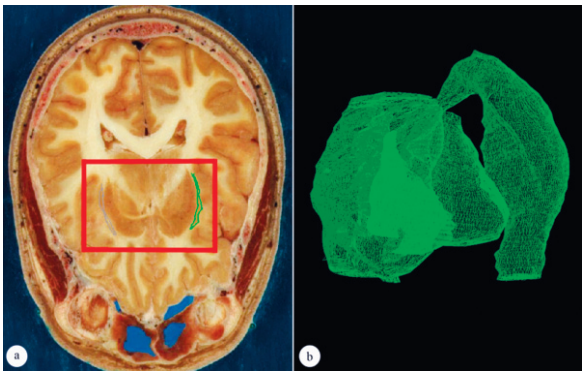

Figure 1. A. Photographic cross-section of the claustra from the Visible Human Male. Surface modelling first involves identifying the region of a desired tissue in the volume and then constructing a description of this region as a surface; **B.** Wireframe reconstruction of the claustra and the surrounding structures. Wireframe models are important in model generation because they lend themselves well to smoothing functions such as lofting, sweeping, and blending.

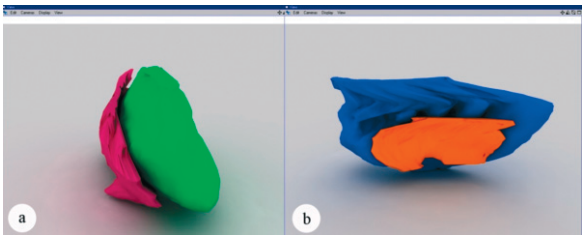

Figure 2. The claustra and surrounding structures are displayed as photorealistic models in different colours to reveal their relationship to each other better; **A.** Claustrum and putamen; **B.** Claustrum and insular cortex.

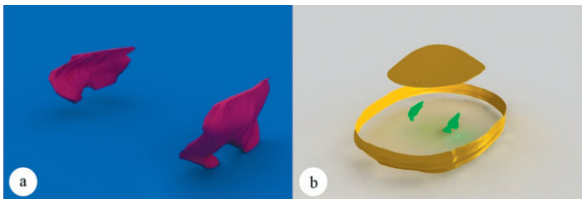

Figure 3. A. A perspective view of photorealistically reconstructed claustra in cinema 4D window; **B.** Spatial location of the both claustra in the cranium, a portion of cranium removed to indicate inside of the cranium.

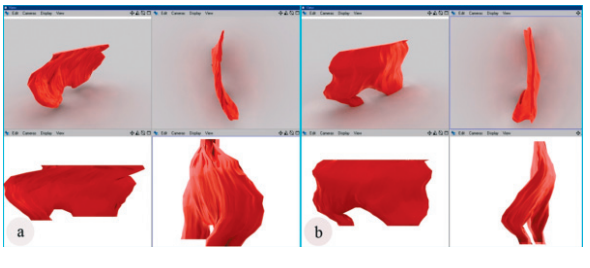

Figure 6. The photorealistic 3D rendered images of the right claustrum (**A**) and left claustrum (**B**) from different angles.

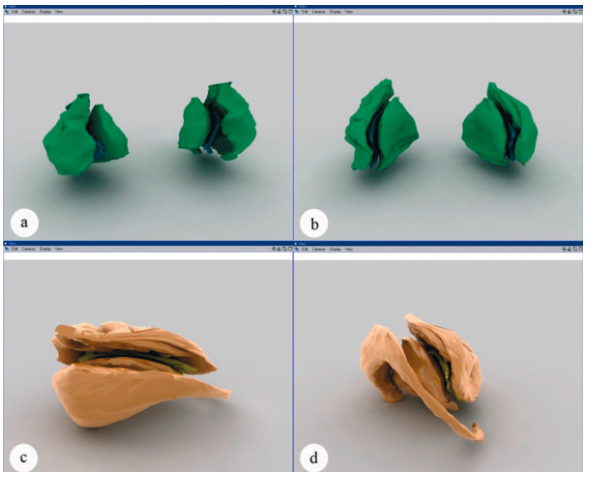

Figure 4. Three-dimensional reconstruction, photorealistic imaging, and spatial relationship of the claustra and surrounding structures. All the anatomical details belonging to the claustra and surrounding structures can be seen with high sensitivity in 3D; **A.** Anterior view of the insular cortex, claustrum, and putamen; **B.** Posterior view of the insular cortex, claustrum, and putamen; **C.** Superior view of the insular cortex, claustrum, putamen, and caudate nucleus; **D.** Supero-posterior view of the insular cortex, claustrum, putamen, and caudate nucleus.

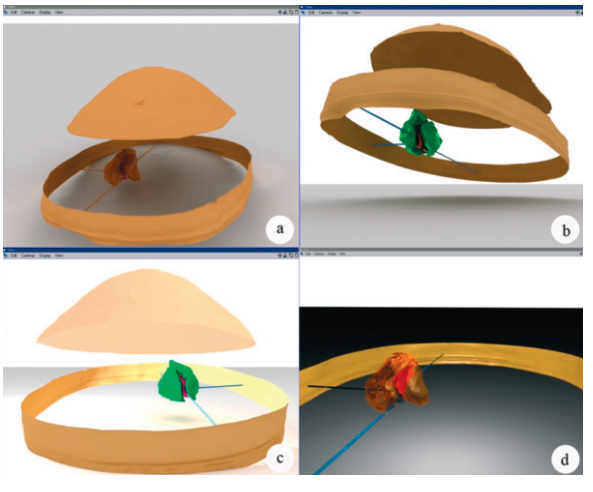

Figure 5. Stereotactic approach is a method developed in order to achieve any destination in the central nervous system by using a 3D coordinate system without damaging the cortical structures. During the application of stereotaxy, the positioning of the lesion at an optimal site is considered essential for clinical diagnosis and treatment; **A.** Anterior view of the insular cortex, claustrum, and putamen; **B.** Antero-inferior view of the insular cortex, claustrum, and putamen; **C.** Posterior view of the insular cortex, claustrum, and putamen with superior illumination; **D.** Anterior view of the insular cortex, claustrum, and putamen, given the opacity to the claustrum and the transparency to the insular cortex and putamen in order to show the passage of the stereotactic instruments.

Many authors using different techniques such as stereology [34], proteomic methods [38], and MRI [19] have all studied the morphology of the claustrum and connections with the surrounding structures. For instance, in Kowianski's et al. study [34] the histological sections were projected onto a sheet of paper and, at the final magnification, depending on the size of the specimen, the outlines of the cortical areas and claustrum were drawn. Almost all of them showed the claustrum as 2D and cross-sectional. At the same time, based on these 2D sections, 3D structures of the claustrum were viewed by drawing. In this study, however, the claustra and the surrounding structures were reconstructed in 3D. In addition, the spatial relationship among the claustra and the surrounding structures were shown both three-dimensionally and photorealistically. Using microscopy techniques, it was reported that the claustrum can be 2 to 4 subdivisions [22, 40, 46]. Also, it was suggested that the claustrum is connected to various brain regions such as the neocortex [43] and entorhinal cortex [41] that are pertinent to some major neurological disorders including those related to aging [39]. However, this macroscopic study does not elucidate the details on the claustral subdivisions and its connections.

This study dealt with morphometric and volumetric evaluation of the claustrum and the surrounding structures, although previous studies almost exclusively measured the volume of the claustrum [19, 34]. Moreover, the spatial location of the claustrum in the skull was defined, and the levels at which the claustrum appeared and disappeared from vertex topographically were determined. The right claustrum was measured as 828.8346 mm^3 and the left claustrum was measured as 705.8160 mm^3 (Table 1). A post-mortem volumetric study by Kowianski et al. [34] reported average human claustral volume to be 580 mm^3, which is considerably smaller than the average claustral volume reported by Davis [19] (701 mm^3 in typically developing boys and 555 mm^3 in boys with autism). Davis [19] reported that there was a significantly smaller claustral volume in individuals with autism. Because the claustrum serves as an integrating centre for all cortical modalities, this smaller claustral volume could be indicative of the under-connectivity found in autism, as has been suggested by Just et al. [19, 27].

There was a significant difference between right and left claustrum volume (right > left; Table 1). It would be more indicative of general hemispheric differences rather than an association with a particular neuropathology [19]. Other brain structures have also been shown to exhibit hemispheric differences, such as the hippocampus [37] and amygdala [49], with the right being larger than the left. Based on possible functions of the claustrum [18], it is unclear why such laterality would exist, but laterality of claustral involvement has been shown in other studies, as well: Bonilha et al. [13] reported increased left claustral volume in a voxel-based morphometry study of young males with autism. Naghavi et al. [44] reported the right claustrum and insula to be increasingly activated with modal sensory integration of conceptually related objects. Lerner et al. [36] reported more right than left claustral activation associated with suppression of natural urges. Olson et al. [47] found left claustral activation in cross-modal integration of audio-visual stimuli. Banati et al. [10] found left claustral activation in response to visual-tactile integration, and Hadjikhani and Roland [24] found right claustrum activation in visual-tactile cross-modal transfer [19].

The claustrum and surrounding structures, due to their spatial position and spatial relationship, considered the subcortical centres, are important in stereotactic surgery. Stereotactic surgery is a minimally invasive form of surgical intervention which makes use of the 3D coordinate system to pinpoint the location of small targets inside the skull and to carry out actions such as biopsies, injections, stimulation, implantation, etc. Stereotactic biopsy is the gold standard to obtain a definite histopathological diagnosis in tumour patients in which complete resection is not feasible or the origin of the lesion is completely unclear [50]. Image-guided neurosurgery is an advancing sub-speciality in neurosurgery [35]; image fusion allows the superimposition of MRI and CT scans to define the target point more accurately, which reduces complications and facilitates safe and effective stereotactic biopsy in virtually any brain area [50]. Failure to obtain a diagnosis (so-called sampling error) commonly occurs because the selected target was in the necrotic centre of a tumour or the enhancing area was missed. Therefore, a low-grade tumour is diagnosed instead of the correct high-grade tumour. Careful preoperative study of the images, double-dose contrast administration, and selection of multiple targets until the attending neuropathologist has received an adequate specimen can obviate these difficulties [50]. Stereotactic biopsy is a procedure with a low mortality rate of less than 0.1% and very low morbidity [5]. Complications include major haemorrhage, seizures, and broken instruments [5]. The introduction of computer-based image-guided stereotactic biopsy has further reduced the complication

rate; the better visualisation of vessels in preoperative trajectory planning can prevent damage which may lead to haemorrhage [50]. The technique used in this study enables us to determine the spatial coordinates of the target tissues and to rehearse the surgical procedures for the preoperative trajectory planning by using virtual surgery. The data obtained from this method can be used to design instruments to be used in the operation.

In summary, there are only a few data in the literature related to the claustrum of the human brain. Additionally, computer-aided 3D reconstructions of the claustra and measurements regarding the dimensions of these structures have not been reported previously. In this study, a feasible, reliable, and valid method for 3D reconstruction from any serial sections or images was presented using a real human cadaver. This technique gives significant unreported information about the dimensions and 3D relationship of the claustrum and surrounding structures. Therefore, this study will be a very useful anatomical guide for neuroscientists and neurosurgeons interested in the claustrum.

REFERENCES

1. Ackerman MJ, Banvard RA (2000) Imaging outcomes from The National Library of Medicine's Visible Human Project. Comput Med Imag Graph, 24: 125–126.
2. Akselrod-Ballin A, Galun M, Gomori JM, Brandt A, Basri R (2007) Prior knowledge driven multiscale segmentation of brain MRI. Med Imag Comput Comput Assist Interv, 10 (Part 2): 118–126.
3. Amaral DG, Cowan WM (1980) Subcortical afferents to the hippocampal formation in the monkey. J Comp Neurol, 189: 573–591.
4. Amaral DG, Insausti R (1992) Retrograde transport of D-[3H]-aspartate injected into the monkey amygdaloid complex. Exp Brain Res, 88: 375–388.
5. Apuzzo ML, Chandrasoma PT, Cohen D, Zee CS, Zelman V (1987) Computed imaging stereotaxy: experience and perspective related to 500 procedures applied to brain masses. Neurosurgery, 20: 930–937.
6. Arikuni T, Kubota K (1985) Claustral and amygdaloid afferents to the head of the caudate nucleus in macaque monkeys. Neurosci Res, 2: 239–254.
7. Ashwell KW, Hardman C, Paxinos G (2004) The claustrum is not missing from all monotreme brains. Brain Behav Evol, 64: 223–241.
8. Baizer JS, Lock TM, Youakim M (1997) Projections from the claustrum to the prelunategyrus in the monkey. Exp Brain Res, 113: 564–568.
9. Ballinger JR (2009) MRI Artefacts. URL:http://www.mritutor.org/mritutor/artifact.htm [accessed July 2011].
10. Banati RB, Goerres GW, Tjoa C, Aggleton JP, Grasby P (2000) The functional anatomy of visual-tactile integration in man: a study using positron emission tomography. Neuropsychologia, 38: 115–124.
11. Bennett CM, Baird AA (2006) Anatomical changes in the emerging adult brain: a voxel-based morphometry study. Human Brain Mappi, 27: 766–777.
12. Berns GS, Chappelow J, Cekic M, Zink CF, Pagnoni G, Martin-Skurski ME (2006) Neurobiological substrates of dread. Science, 312: 754–758.
13. Bonilha L, Cendes F, Rorden C, Eckert M, Dalgalarrondo P, Li LM, Steiner CE (2008) Gray and white matter imbalance — typical structural abnormality underlying classic autism? Brain Dev, 30: 396–401.
14. Butler AB, Molnár Z, Manger PR (2002) Apparent absence of claustrum in monotremes: implications for forebrain evolution in amniotes. Brain Behav Evol, 60: 230–240.
15. Chachich ME, Powell DA (2004). The role of claustrum in Pavlovian heart rate conditioning in the rabbit (Oryctolagus cuniculus): anatomical, electrophysiological, and lesion studies. Behav Neurosc, 118: 514–525.
16. Corso JJ, Tu Z, Yuille A, Toga A (2007) Segmentation of sub-cortical structures by the graph-shifts algorithm. Inf Process Med Imag, 20: 183–197.
17. Crick FC (1994) The astonishing hypothesis. Charles Scribner's Sons, New York.
18. Crick FC, Koch C (2005). What is the function of the claustrum? Philos Trans R Soc Lond B Biol Sci, 360: 1271–1279.
19. Davis WB (2008) The claustrum in autism and typically developing male children: a quantitative MRI study. Young University, Brigham.
20. Dubroff JG, Ficicioglu C, Segal S, Wintering NA, Alavi A, Newberg AB (2008) FDG-PET findings in patients with galactosaemia. J Inherited Metab Dis, 31: 533––539.
21. Edelstein LR, Denaro FJ (2004) The claustrum: a historical review of its anatomy, physiology, cytochemistry and functional significance. Cell Mol Biol (Noisy-legrand), 50: 675–702.
22. Fernández-Miranda JC, Rhoton AL Jr, Kakizawa Y, Choi C, Alvarez-Linera J (2008). The claustrum and its projection system in the human brain: a microsurgical and tractographic anatomical study. J Neurosurg, 108: 764–774.
23. Geiger B (1993) Three dimensional modeling of human organs and its application to diagnosis and surgical planning, Ph.D. Theses, INRIA, France.
24. Hadjikhani N, Roland PE (1998) Cross-modal transfer of information between the tactile and the visual representations in the human brain: a positron emission tomographic study. J Neurosci, 18: 1072–1084.
25. Haines DE (2000) Neuroanatomy: an atlas of structures, sections, and systems. 5th Ed. Lippincott Williams and Williams, Philadelphia, PA.
26. Insausti R, Amaral DG, Cowan WM (1987) The entorhinal cortex of the monkey: III. Subcortical afferents. J Comp Neurol, 264: 396–408.
27. Just MA, Cherkassky VL, Keller TA, Kana RK, Minshew NJ (2007) Functional and anatomical cortical underconnectivity in autism: evidence from an FMRI study of an

executive function task and corpus callosum morphometry. Cereb Cortex, 17: 951–961.
28. Kalaitzakis ME, Christian LM, Moran LB, Graeber MB, Pearce RK, Gentleman SM (2009) Dementia and visual hallucinations associated with limbic pathology in Parkinson's disease. Parkinsonism Relat Disord, 15: 196––204.
29. Kalaitzakis ME, Graeber MB, Gentleman SM, Pearce RK (2008) Striatal beta-amyloid deposition in Parkinson disease with dementia. J Neuropathol Exp Neurol, 67: 155–161.
30. Kalaitzakis ME, Pearce RK, Gentleman SM (2009) Clinical correlates of pathology in the claustrum in Parkinson's disease and dementia with Lewy bodies. Neurosci Lett, 461: 12–15.
31. Kapakin S (2011) Stereolithographic biomodelling to create tangible hard copies of the ethmoidal labyrinth air cells based on the visible human project. Folia Morphol, 70: 33–40.
32. Kapakin S, Demiryurek D (2009) The reproduction accuracy for stereolithographic model of the thyroid gland derived from the visible human dataset. Saudi Med J, 30: 887–892.
33. Kievit J, Kuypers HG (1975) Subcortical afferents to the frontal lobe in the rhesus monkey studied by means of retrograde horseradish peroxidase transport. Brain Res, 85: 261–266.
34. Kowiański P, Dziewiatkowski J, Kowiańska J, Moryś J (1999) Comparative anatomy of the claustrum in selected species: a morphometric analysis. Brain Behav Evol, 53: 44–54.
35. Lee JY, Lunsford LD, Subach BR, Jho HD, Bissonette DJ, Kondziolka D (2000). Brain surgery with image guidance: current recommendations based on a 20-year assessment. Stereotact Funct Neurosurg, 75: 35–48.
36. Lerner A, Bagic A, Hanakawa T, Boudreau EA, Pagan F, Mari Z, Bara-Jimenez W, Aksu M, Sato S, Murphy DL, Hallett M (2009) Involvement of insula and cingulate cortices in control and suppression of natural urges. Cereb Cortex, 19: 218–223.
37. Li YJ, Ga SN, Huo Y, Li SY, Gao XG (2007) Characteristics of hippocampal volumes in healthy Chinese from MRI. Neurol Res, 29: 803–806.
38. Mathur BN, Caprioli RM, Deutch AY (2009) Proteomic analysis illuminates a novel structural definition of the claustrum and insula. Cereb Cortex, 19: 2372–2379.
39. Moryś J, Berdel B, Maciejewska B, Król J, Dziewiatkowski J (1996) Loss of neurons in the claustrum of aging brain. Folia Neuropathol, 34: 97–101.
40. Moryś J, Berdel B, Maciejewska B, Sadowski M, Sidorowicz M, Kowiańska J, Narkiewicz O (1996) Division of the human claustrum according to its architectonics and morphometric parameters. Folia Morphol, 55: 69–82.
41. Moryś J, Bobiński M, Kozłowski P, Dziewiatkowski J, Switka A, Wiśniewski H, Narkiewicz O (1993) The pathology of the claustrum in Galloway syndrome indicates the existence of claustro-entorhinal pathway. Folia Morphol, 52: 1–9.
42. Morys J, Bobinski M, Wegiel J, Wisniewski HM, Narkiewicz O (1996) Alzheimer's disease severely affects areas of the claustrum connected with the entorhinal cortex. Journal fur Hirnforschung, 37: 173–180.
43. Morys J, Narkiewicz O, Wisniewski HM (1993) Neuronal loss in the human claustrum following ulegyria. Brain Res, 616: 176–180.
44. Naghavi HR, Eriksson J, Larsson A, Nyberg L (2007) The claustrum/insula region integrates conceptually related sounds and pictures. Neurosci Lett, 422: 77–80.
45. Naqvi NH, Rudrauf D, DamasioH, Bechara A (2007) Damage to the insula disrupts addiction to cigarette smoking. Science, 315: 531–534.
46. Navamar MR, Sadeghi Y, Haghir H (2005) A new division of the human claustrum basis on the anatomical landmarks and morphological findings. J Iran Anat Scien, 3: 57–66.
47. Olson IR, Gatenby JC, Gore JC (2002). A comparison of bound and unbound audio-visual information processing in the human cerebral cortex. Brain Res Cogn Brain Res, 14: 129–138.
48. Pearson RC, Brodal P, Gatter KC, Powell TP (1982) The organization of the connections between the cortex and the claustrum in the monkey. Brain Res, 234: 435––441.
49. Pedraza O, Bowers D, Gilmore R (2004) Asymmetry of the hippocampus and amygdala in MRI volumetric measurements of normal adults. J Int Neuropsychol Soc, 10: 664–678.
50. Setzer M, Herminghaus S, Marquardt G, Tews DS, Pilatus U, Seifert V, Zanella F, Lanfermann H (2007) Diagnostic impact of proton MR-spectroscopy versus image-guided stereotactic biopsy. Acta Neurochir, 149: 379–386.
51. Shipp S, Blanton M, Zeki S (1998) A visuo-somatomotor pathway through superior parietal cortex in the macaque monkey: cortical connections of areas V6 and V6A. Eur J Neurosci, 10: 3171–3193.
52. Sperner J, Sander B, Lau S, Krude H, Scheffner D (1996) Severe transitory encephalopathy with reversible lesions of the claustrum. Pediatric Radiol, 26: 769–771.
53. Spitzer V, Ackerman MJ, Scherzinger AL, Whitlock D (1996) The visible human male: a technical report. JAMIA, 3: 118–130.
54. Stein MB, Simmons AN, Feinstein JS, Paulus MP (2007) Increased amygdala and insula activation during emotion processing in anxiety-prone subjects. Am J Psychiatry, 164: 318–327.
55. Uzunbaş MG, Soldea O, Unay D, Cetin M, Unal G, Erçil A, Ekin A (2010) Coupled nonparametric shape and moment-based intershape pose priors for multiple basal ganglia structure segmentation. IEEE Trans Med Imag, 29: 1959–1978.
56. Webster MJ, Bachevalier J, Ungerleider LG (1993) Subcortical connections of inferior temporal areas TE and TEO in macaque monkeys. J Comp Neurol, 335: 73–91.
57. Yang J, Staib LH, Duncan JS (2004) Neighbor-constrained segmentation with level set based 3-D deformable models. IEEE Trans Med Imag, 23: 940–948.
58. Zhang X, Hannesson DK, Saucier DM, Wallace AE, Howland J, Corcoran ME (2001) Susceptibility to kindling and neuronal connections of the anterior claustrum. J Neurosc, 21: 3674–3687.